Theor Chem Acc (2009) 124:49–57
DOI 10.1007/s00214-009-0579-z

REGULAR ARTICLE

Computational study of the substitution effect on the mechanism for phospha-Wittig reaction

Hsin-Yi Liao

Received: 20 January 2009 / Accepted: 29 April 2009 / Published online: 16 May 2009

Abstract The phospha-Wittig reaction HP=PH$_3$ + O=CHX → HP=CHX + O=PH$_3$ (X = H, F, Cl, Me, OMe, NMe$_2$, CMe$_3$) was examined using the density functional theory calculations. All of the structures were completely optimized at the B3LYP/6-311++G** level of theory. The reactivities of various O=CHX were examined by estimating their activation energies. The main finding of this work is that the configuration mixing model can successfully predict the relative ordering of the activation energy and reaction enthalpies of the phospha-Wittig reaction. It was demonstrated that O=CHX with more electro-releasing substituents will possess a smaller singlet–triplet splitting. This will facilitate the phospha-Wittig reaction and will result in a larger exothermicity.

Keywords Phospha-Wittig reaction · Density functional theory · Configuration mixing (CM) model · Singlet–triplet splitting

1 Introduction

The Wittig reaction is one of the important methods for the synthesis of carbon–carbon double bond [1–3]. Alkylidenephosphoranes ($R'_2C{=}PR_3$), or called phosphorus ylides, are useful in reacting with a carbonyl compound to form an olefin and a phosphine oxide so as to be termed as Wittig reagents. Ylides are dipolar molecules that contain positive and negative charges on adjacent atoms. The phosphorus ylide can be viewed as a carbanion directly attached to a phosphorus atom carrying a substantial degree of positively charge [4].

Since there is an carbon–phosphorus diagonal relationship widespread recognized [5], the last 20 years has seen efforts to extend the Wittig reagents to include the phospha-Wittig reagent, which is the phosphorus analog of the Wittig reagent [6]. In 1988, Mathey et al. utilized transition metals and complexation to devise the phospha-Wittig reagent $[(R'O_2)P(O){-}P^{-}R]W(CO)_5$ [7–9]. More recently, the so-called free phosphanylidene-σ^4-phosphoranes ArP=PR$_3$ were prepared [10]. According to Protasiewicz et al., phosphoranylidenephosphines DmpP=PMe$_3$ (Dmp = 2,6-Mes$_2$C$_6$H$_3$) and Mes*P=PMe$_3$ (Mes* = 2,4,6-$Bu^t_3C_6H_2$) can act as the phospha-Wittig reagents to react with aldehydes to form phosphaalkenes [ArP=C(H)R] and phosphine oxides in high yields (Eq. 1) [11].

$$ArP{=}PMe_3 + O{=}C(H)R \rightarrow ArP{=}C(H)R + O{=}PMe_3. \qquad (1)$$

When DmpP=PMe$_3$ and Mes*P=PMe$_3$ react with various aldehydes, Protasiewicz found that the reaction times and product yields varied with the nature of the substituent of the aldehydes [11]. In addition, each reaction exclusively produced *E*-isomers of the phosphaalkene. Further, reaction of DmpP=PMe$_3$ with ketone showed no evidence of phosphaalkene formation [11]. Meanwhile, no ^{31}P-NMR resonances, which indicate the presence of betaine-like intermediates, have been detected [6]. Thus, a similar mechanism as proposed for the Wittig reaction is suggested.

Many studies concerning the mechanism and stereochemistry for the Wittig reaction have been conducted by theoretical and experimental chemists [12–21]. There is evidence that phosphorus ylides can react with carbonyl

---

H.-Y. Liao (✉)
Department of Science Education,
National Taipei University of Education,
Taipei 10659, Taiwan
e-mail: hyliao@tea.ntue.edu.tw

compounds via a concerted or nearly concerted cycloaddition to directly form a four-membered oxaphosphatanes in vacuum [22]. Then, an elimination step from the oxaphosphatanes forms the final products.

There are so far several synthetic applications of the phospha-Wittig reaction [23–29]. However, to the best of our knowledge, this is the first computational report concerning a systematic study of the substitution effect on the mechanism for the phospha-Wittig reaction based on the more sophisticated theory. Therefore, in this study we report a theoretical investigation of phospha-Wittig gas-phase reactions using the density functional theory calculations. The system we choose to study are the addition of HP=PH_3 to O=CHX (X = H, F, Cl, Me, OMe, NMe_2, CMe_3).

The primary purpose of this study is to provide a systematic theoretical study of the energy profiles for this reaction and to systematically elucidate the changes in the kinetic and thermodynamic properties of the phospha-Wittig reaction when the phospha-Wittig reagent reacts with various C=O containing molecules. We would like to demonstrate that the reactivity of O=CHX is strongly correlated to its singlet–triplet splitting (ΔE_{ST}). These results will provide insight into the driving force for the phospha-Wittig reactions.

2 Methodology

The geometries of reactants, intermediates, transition states, and products were fully optimized using the hybrid density functional B3LYP method, i.e., Becke's three-parameter functional [30–32] with the correlation functional of Lee et al. [33], with the 6-311++G** basis set [34, 35]. Vibrational frequencies, also calculated at the B3LYP/6-311++G** level of theory, were used for characterization of stationary points. All of the stationary points were positively identified for minima (number of imaginary frequencies, NIMAG = 0) or transition states (NIMAG = 1). All calculations were performed with the GAUSSIAN 03 package [36]. Zero-point vibrational energies (ZPE) were included in the reported energies.

Orbital energies were determined at the HF/6-311++G** level of theory. It is known that the HF results are a useful reference for comparing the experimental results according to Koopmans' theorem [37, 38]. In addition, the orbitals and charges were analyzed by means of the natural bond orbital (NBO) scheme [39].

To consider the solvent effect on the phospha-Wittig reaction, the self-consistent isodensity polarizable continuum model (SCI-PCM) [40] was applied. Tetrahydrofuran (THF) is chosen as the solvent in this study because it is one of the most common solvents used in Wittig or phospha-Wittig reactions. The dielectric constant ε is set to 7.58, which is the default value in GAUSSIAN 03 package.

3 Results and discussion

The results for five regions on the energy profiles are presented here: the reactant (HP=PH_3 + O=CHX; **R**), the transition state for complexation (**TS-C**), the intermediate (**IM**), the transition state for decomposition (**TS-D**), and the product (HP=CHX + O=PH_3; **P**). The energy profile for X = H is shown in Fig. 1. As shown in Fig. 1, addition of phosphorus ylide to formaldehyde leads to the formation of an intermediate via a four-center approach. Then, the second transition state (**TS-D**) is characterized as the

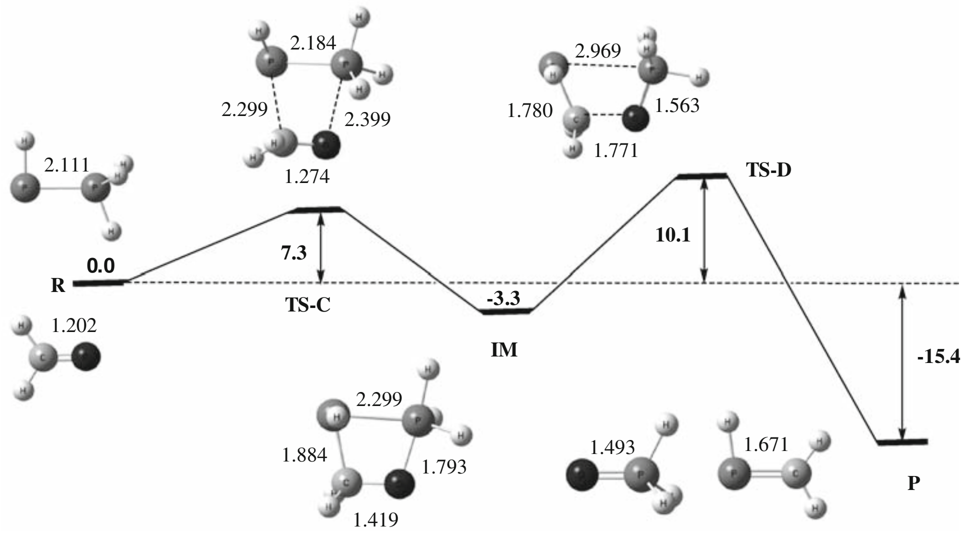

Fig. 1 Energy profile for the phospha-Wittig reaction of HP=PH_3 and O=CH_2. The relative energies (in kcal/mol) and all bond distances (in Å) are calculated at the B3LYP/6-311++G** level of theory

decomposition of the intermediate which leads to the formation of phosphaalkene ($HP{=}CH_2$) and phosphine oxide ($O{=}PH_3$).

The four-center transition state for complexation (**TS-C**) has a slightly asynchronous character. The newly formed P–C and P–O bond distances are 2.299 and 2.399 Å, respectively. When comparing $d(\mathrm{P–C}) = 1.884$ Å and $d(\mathrm{P–O}) = 1.793$ Å for **IM**, the **IM** is formed by a concerted, asynchronous, double nucleophilic addition of P to C then O to P (see **1** for charges on each atoms in **R**).

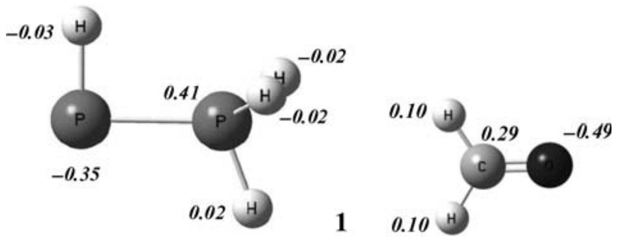

1

In the **TS-C** and **IM**, the geometry around carbon is changed from planar triangular shape to tetrahedron (i.e. rehybridization from sp^2 to sp^3 on the carbon center). In addition, the C=O bond distances are both lengthened when compared to the formaldehyde. That is, the formaldehyde moiety in the **TS-C** and **IM** resemble more closely to the triplet formaldehyde than the singlet one. Thus, we suggest that the triplet $O{=}CH_2$ is involved in the reaction, in other words, the $O{=}CH_2$ can be imagined to present in the triplet valence state with both HOMO (LP(O)) and LUMO (π^*(C=O)) singly occupied (see Fig. 2). To be consistent, ylide partner should also exist in the triplet valence state, thus the formation of the two new σ bonds between the two moieties is feasible and the reaction system can keep in the singlet state. Furthermore, the transition state for decomposition shows synchronously bond cleavage.

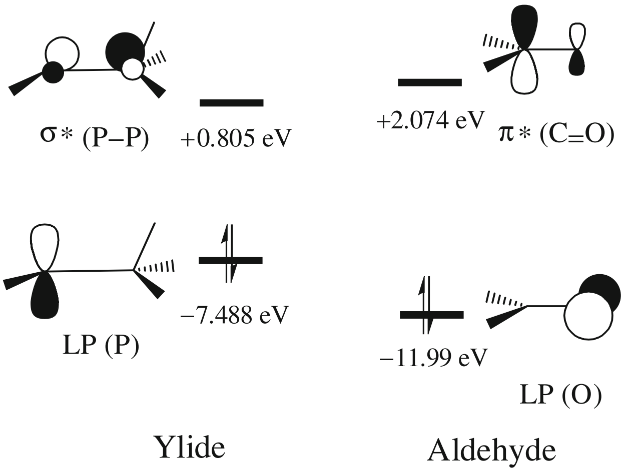

Fig. 2 Frontier orbitals for the phosphorus ylide and formaldehyde. The orbital energies (in eV) are calculated at the HF/6-311++G** level of theory

The energy profile of the reaction shows that the barrier height for complexation is lower than that of decomposition. In addition, the energy of the **IM** relative to its reactants is quite small (−3.3 kcal/mol) and the reaction is 15.4 kcal/mol exothermic at the B3LYP/6-311++G** level of theory.

In this study, different substituents on OCHX are used to understand the factors affecting the phospha-Wittig reaction. The geometrical parameters, charges and orbital energies for OCHX (X = H, F, Cl, Me, OMe, NMe_2, CMe_3) are listed in Table 1. As shown in Table 1, when X is an electron-releasing group (X = Me, CMe_3, NMe_2), the C=O bond distance is lengthened as the energy of HOMO (n(O)) is raising. That is, the more electron-releasing ability, the longer d(C=O). X = NMe_2 is the most electron-releasing group and thus $OCH(NMe_2)$ has the longest C=O bond. Whereas, when X is an electron-withdrawing group (X = OMe, Cl, F), the C=O bond distance is shorter than that of X = H and the energy of HOMO (n(O)) is lower than that of X = H. For example, OCHF has the shortest $d(\mathrm{C{=}O}) = 1.177$ Å.

When OCHX is used in the phospha-Wittig reaction, two isomers (*E*/*Z* isomers) of the phosphaalkene are possibly formed. The fully optimized geometries for these stationary points calculated at the B3LYP/6-311++G** level of theory are given in Figs. 3, 4, and 5, respectively. The corresponding relative energies at the B3LYP/6-311++G** level of theory are collected in Table 2. The energy profiles for the more exothermic isomer for each substituent are summarized in Fig. 6.

As can be seen in Table 2, reaction paths forming the *Z* isomers of the phosphaalkenes are more thermodynamically stable except X = CMe_3 and NMe_2. For simplifying our discussion, we focus on the paths with the more exothermic isomers since the energy differences between these two pathways for respective substituents are not significant. As

Table 1 B3LYP/6-311++G** calculated C=O bond distances [d(C=O), in Å], atomic charges (q) (NBO charges) and orbital energies (in eV) (RHF/6-311++G** calculated results) for OCHX [X = H, F, Cl, CH_3, OCH_3, $N(CH_3)_2$, $C(CH_3)_3$]

X	d(C=O)	q(C)	q(O)	n(O)	π^*(C=O)
H	1.202	0.29	−0.49	−11.99	2.074
CH_3	1.206	0.44	−0.52	−11.55	1.803
$C(CH_3)_3$	1.205	0.46	−0.53	−11.11	1.492
$N(CH_3)_2$	1.217	0.54	−0.62	−10.27	1.684
H	1.202	0.29	−0.49	−11.99	2.074
OCH_3	1.201	0.66	−0.58	−12.69	2.038
Cl	1.179	0.39	−0.46	−12.89	2.287
F	1.177	0.74	−0.49	−14.01	2.318

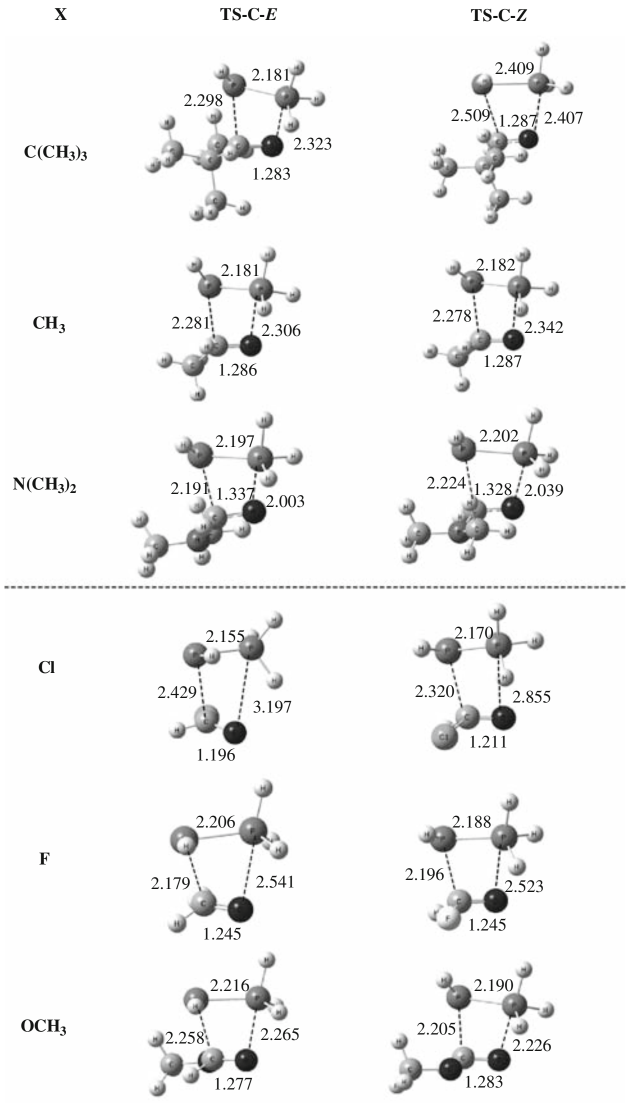

Fig. 3 B3LYP/6-311++G** optimized geometries (in Å) of the transition states for complexation (**TS-C**). Structures *above the dashed lines* are with the electron-releasing groups and *below* are with the electron-withdrawing groups

shown in Fig. 3, the C=O double bond of **TS-C** is stretched by 2.7, 5.8, 6.5, 6.7, 6.8, 9.7% for X = Cl, F, CMe$_3$, Me, OMe, and NMe$_2$, respectively, relative to its value of corresponding OCHX. This feature indicates that the transition state structures with the smaller C=O double bond stretch show more reactant-like character. That is, the barrier is encountered earlier in the reaction. Consequently, the order of barrier height for **TS-C** follows the trend as this C=O double bond stretch (Table 2): Cl (5.1 kcal/mol) < F (9.1 kcal/mol) < CMe$_3$ (11.3 kcal/mol) < Me (12.3 kcal/mol) < OMe (19.8 kcal/mol) < NMe$_2$ (21.4 kcal/mol). This is consistent with the Hammond's postulate [41], which associates an earlier transition state with a smaller barrier and a more exothermic reaction.

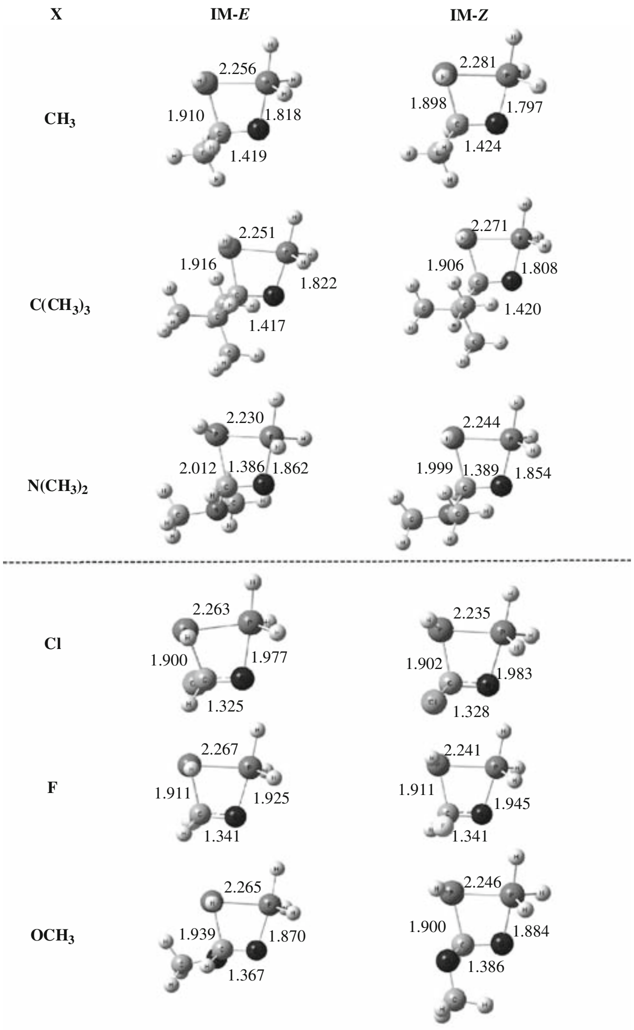

Fig. 4 B3LYP/6-311++G** optimized geometries (in Å) of the intermediates (**IM**). Structures *above the dashed lines* are with the electron-releasing groups and *below* are with the electron-withdrawing groups

The optimized intermediate geometries (**IM**) are collected in Fig. 4. The bond distances of two newly formed bonds in the **TS-C** are stretched on average by 33, 25, 24, 22, 17, and 8% relative to their corresponding **IM** equilibrium values for X = Cl, Me, CMe$_3$, F, OMe, and NMe$_2$, respectively. The more the bond stretch, the earlier is the transition state, i.e., the more exothermic intermediate. Thus, the order of exothermicity is anticipated to follow the same trend as the percentage of bond stretch: X = Cl (2.6 kcal/mol) < Me (2.8 kcal/mol) < CMe$_3$ (3.3 kcal/mol) < F (6.0 kcal/mol) < OMe (17.7 kcal/mol) < NMe$_2$ (21.3 kcal/mol).

As we stated earlier, comparing the structures of **IM** and their corresponding isolated reactants, we found that the geometrical parameters of OCHX moiety in the **IM** resemble more closely to those of the triplet OCHX. This implies that

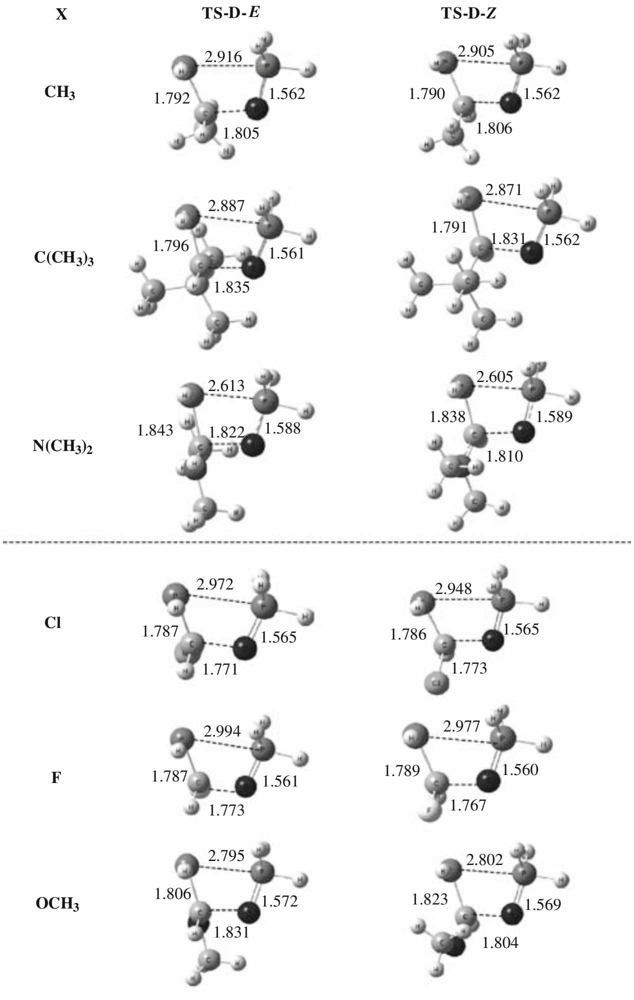

Fig. 5 B3LYP/6-311++G** optimized geometries (in Å) of the transition states for decomposition (**TS-D**). Structures *above the dashed lines* are with the electron-releasing groups and below are with the electron-withdrawing groups

Table 2 B3LYP/6-311++G** calculated singlet–triplet splittings (ΔE_{ST}, in kcal/mol) for OCHX and relative energies (in kcal/mol) for the reaction of HP=PH$_3$ + OCHX → HP=CHX + O=PH$_3$ [X = H, F, Cl, CH$_3$, OCH$_3$, N(CH$_3$)$_2$, C(CH$_3$)$_3$]

X	E_a-C[a]	ΔE-IM[b]	E_a-D[c]	ΔE[d]	ΔE_{ST}[e]
H	7.3	−3.3	10.1	−15.4	65.5
CH$_3$					
E	11.3	3.2	16.6	−9.1	71.6
Z	*12.3*	*2.8*	*16.4*	*−9.3*	
C(CH$_3$)$_3$					
E	*11.3*	*3.3*	*18.5*	*−8.1*	70.7
Z	12.8	3.8	18.6	−7.7	
N(CH$_3$)$_2$					
E	*21.4*	*21.3*	*27.1*	*0.3*	85.5
Z	22.6	21.9	28.3	1.3	
Cl					
E	2.8	2.8	24.6	−2.1	81.5
Z	*5.1*	*2.6*	*24.8*	*−2.6*	
F					
E	10.0	6.6	27.6	5.3	93.3
Z	*9.1*	*6.0*	*28.1*	*5.2*	
OCH$_3$					
E	21.0	17.5	29.6	7.0	95.3
Z	*19.8*	*17.7*	*32.1*	*6.6*	

Values in italics indicate the data for the more stable isomer

[a] $E_a\text{-C} = E[\mathbf{TS\text{-}C}] - E[\mathrm{HP{=}PH_3}] - E[\mathrm{OCHX}]$

[b] $\Delta E\text{-IM} = E[\mathbf{IM}] - E[\mathrm{HP{=}PH_3}] - E[\mathrm{OCHX}]$

[c] $E_a\text{-D} = E[\mathbf{TS\text{-}D}] - E[\mathrm{HP{=}PH_3}] - E[\mathrm{OCHX}]$

[d] $\Delta E = E[\mathrm{HP{=}CHX}] + E[\mathrm{O{=}PH_3}] - E[\mathrm{HP{=}PH_3}] - E[\mathrm{OCHX}]$

[e] $\Delta E_{\mathrm{ST}} = E(\mathrm{triplet}) - E(\mathrm{singlet})$. A positive value indicate a singlet ground state

the triplet OCHX takes part in the singlet energy profile during the phospha-Wittig reaction. Therefore, we calculate the singlet–triplet splittings (ΔE_{ST}) for each OCHX (X = H, F, Cl, Me, OMe, NMe$_2$, CMe$_3$) (see Table 2). The B3LYP/6-311++G** calculations show an increasing trend in ΔE_{ST} for X = H (65.5 kcal/mol) < Me (71.6 kcal/mol) ≈ CMe$_3$ (70.7 kcal/mol) < NMe$_2$ (85.5 kcal/mol) < Cl (81.5 kcal/mol) < F (93.3 kcal/mol) < OMe (95.3 kcal/mol). That is, OCHX with more electro-releasing substituents will possess a smaller singlet–triplet splitting.

We found that this trend is in accordance with that of relative energy for the **IM**, which is X = electron-releasing group: H (−3.3 kcal/mol) < Me (2.8 kcal/mol) < CMe$_3$ (3.3 kcal/mol) < NMe$_2$ (21.3 kcal/mol) and X = electron-withdrawing group: H (−3.3 kcal/mol) < Cl (2.6 kcal/mol) < F (6.0 kcal/mol) < OMe (17.7 kcal/mol). This feature reminds us of the configuration mixing (CM) model [42]. The CM model shows that the barrier height and the reaction enthalpy are strongly influenced by the combined effect of two singlet–triplet splittings for each of the reactants of the reaction. Since ΔE_{ST} for phosphorus ylide is constant, a smaller value of ΔE_{ST} for OCHX is expected to reduce the reaction barrier and to produce a larger exothermicity [43]. All of our computational results are in excellent agreement with the CM model. First, when we observe the trend in relative energy for the products (ΔE), there is a reasonable correlation between the ΔE and the ΔE_{ST} values. As shown in Fig. 7, $\Delta E = 0.6866 \times \Delta E_{\mathrm{ST}} - 58.6$ ($R^2 = 0.9815$ from linear regression). A smaller ΔE_{ST} value corresponds to a larger exothermicity. OCHX with a more electro-releasing substituent, which possesses a smaller singlet–triplet splitting, will facilitate the phospha-Wittig reaction and will result in a larger exothermicity.

Second, as can be seen from Table 2, the activation energies for complexation and for decomposition can also be rationalized using the CM model: when X = electron-releasing group: H (7.3, 10.1 kcal/mol) < Me (12.3,

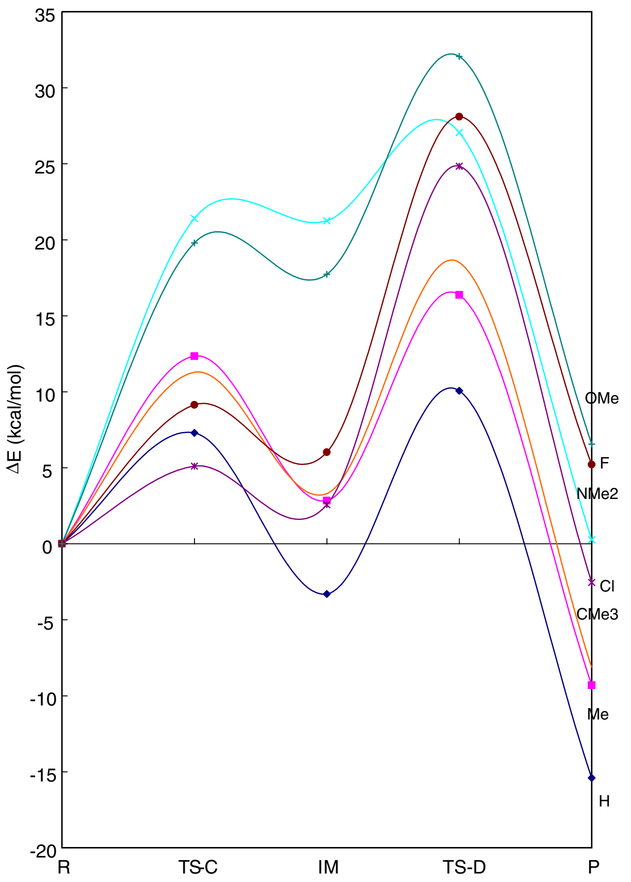

Fig. 6 B3LYP/6-311++G** calculated energy profiles for the phospha-Wittig reactions of the phosphorus ylides with OCHX [X = H, F, Cl, CH_3, OCH_3, $N(CH_3)_2$, $C(CH_3)_3$]

16.4 kcal/mol) ≈ CMe_3 (11.3, 18.5 kcal/mol) < NMe_2 (21.4, 27.1 kcal/mol) and X = electron-withdrawing group: H (7.3, 10.1 kcal/mol) < Cl (5.1, 24.8 kcal/mol) < F (9.1, 28.1 kcal/mol) < OMe (19.8, 32.1 kcal/mol). This investigation provides evidence that the singlet–triplet splitting can be used as a guide to predict the reactivity for different substituents. These results also suggest that the complexation step contained in the mechanism is just like a cycloaddition process. According to our previous study [43], the computational study on the cycloaddition reactions of ethylene with 1,3-dipoles showed that the singlet–triplet splitting of the reactants is the key factor determining the trend of the activation barrier and the reaction enthalpy. We can also observe that the similar trends occurred in the present study and the CM model is verified as a useful tool to describe the reaction involving cycloaddition–reversion processes.

To validate the system $HP{=}PH_3 + O{=}CHX$ as a reasonable model used in describing the experimentally found phospha-Wittig reaction ($ArP{=}PMe_3 + O{=}C(H)R \rightarrow ArP{=}C(H)R + O{=}PMe_3$ [11]), $HP{=}PH_3$ is replaced by $PhP{=}PMe_3$ and an additional X = Ph is calculated to observe the trend discussed above. The relative energies for the products are collected in Table 3. As can be seen in Table 3, comparing to the system of $HP{=}PH_3$ as the reactant (see Table 2), the $PhP{=}PMe_3 + O{=}CHX$ has a larger exothermicity for respective X, and there is still a correlation between the ΔE and the ΔE_{ST} values ($\Delta E = 0.7089 \times \Delta E_{ST} - 70.0$, $R^2 = 0.9639$ from linear regression). Therefore, we suggest that $HP{=}PH_3 + O{=}CH_2$ is a reasonable and efficient model system to discuss the energy profile for the phospha-Wittig reaction.

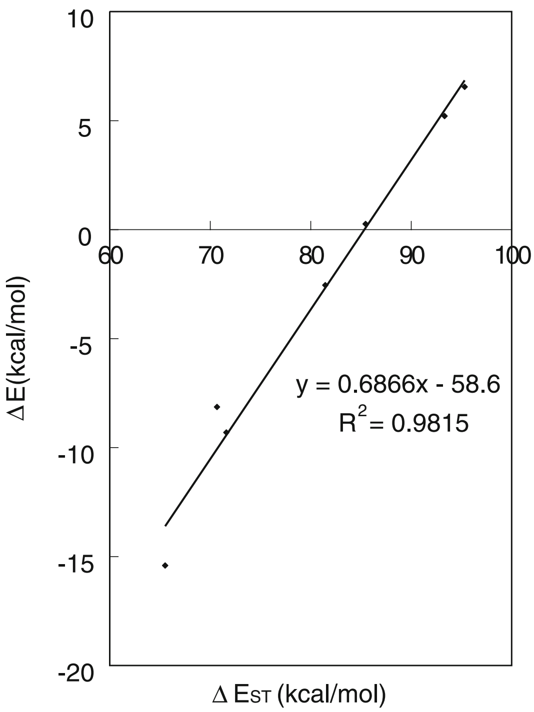

Fig. 7 The correlation between relative energy for the products (ΔE) and ΔE_{ST} of OCHX [X = H, F, Cl, CH_3, OCH_3, $N(CH_3)_2$, $C(CH_3)_3$] at B3LYP/6-311++G** level of theory

As for the stereoselectivity, we found that OCHX with the larger substituent (X = CMe_3 and NMe_2) prefer the *E*-form products. This conclusion is consistent with the experimentally known phospha-Wittig reactions [11]. The phosphorus ylide can be viewed as a donor–acceptor complex with the orbital interaction as shown in **2** [4]. When OCHX with a small substituent approaches the phosphorus ylide, the substituent will be *trans* to the lone pairs so as to reduce the electrostatic repulsion. Whereas, when OCHX with a large substituent approaches the phosphorus ylide, the substituent will prefer the position *trans* to the P–H bond so as to reduce the steric hindrance. Thus, when $HP{=}PH_3$ is replaced by $PhP{=}PMe_3$ (see Table 3), all substituent (except X = OMe) prefer the *E*-form products. We can also realize when $DmpP{=}PMe_3$ and $Mes^*P{=}PMe_3$ react with aldehydes, Protasiewicz found that each reaction exclusively produced *E*-isomers of the phosphaalkene [11].

Table 3 B3LYP/6-311++G** calculated singlet–triplet splittings (ΔE_{ST}, in kcal/mol) for OCHX and relative energies for the products (ΔE, in kcal/mol) for the reaction of PhP=PMe$_3$ + OCHX → PhP=CHX + O=PMe$_3$ [X = H, Ph, F, Cl, CH$_3$, OCH$_3$, N(CH$_3$)$_2$, C(CH$_3$)$_3$]

X	ΔE^{a}	$\Delta E_{\mathrm{ST}}^{b}$
H	−26.6	65.5
Ph		
E	*−20.8*	65.7
Z	−17.2	
CH$_3$		
E	*−19.6*	71.6
Z	−18.3	
C(CH$_3$)$_3$		
E	*−18.7*	70.7
Z	−13.2	
N(CH$_3$)$_2$		
E	*−8.7*	85.5
Z	−3.9	
Cl		
E	*−12.7*	81.5
Z	−12.1	
F		
E	*−4.3*	93.3
Z	−4.1	
OCH$_3$		
E	−2.0	95.3
Z	*−2.2*	

Values in italics indicate the data for the more stable isomer

[a] $\Delta E = E$[PhP=CHX] + E[O=PMe$_3$] − E[PhP=PMe$_3$] − E[OCHX]

[b] $\Delta E_{\mathrm{ST}} = E$(triplet) − E(singlet). A positive value indicate a singlet ground state

In addition, we examined the reaction of HP=PH$_3$ with OC(CH$_3$)$_2$. Comparing to the energy profile of HP=PH$_3$ + OCH(CH$_3$) (as can be seen in Table 4), we found that the reaction of HP=PH$_3$ with OC(CH$_3$)$_2$ is both kinetically and thermodynamically unfavorable because of the larger ΔE_{ST}. Therefore, we can realize when DmpP=PMe$_3$ reacts with ketone, there is no evidence of phosphaalkene formation [11].

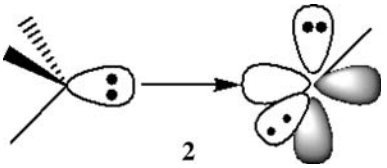

2

Table 4 B3LYP/6-311++G** calculated singlet–triplet splittings (ΔE_{ST}, in kcal/mol) for OCXY and relative energies (in kcal/mol) for the reaction of HP=PH$_3$ + OCXY → HP=CXY + O=PH$_3$ [X = CH$_3$; Y = H, CH$_3$]

OCXY	E_{a}-C^{a}	ΔE-IM^{b}	E_{a}-D^{c}	ΔE^{d}	$\Delta E_{\mathrm{ST}}^{e}$
OC(CH$_3$)$_2$	15.61	7.77	21.18	−4.89	74.50
CH$_3$					
E	11.33	3.24	16.64	−9.06	71.61
Z	*12.34*	*2.83*	*16.37*	*−9.31*	

Values in italics indicate the data for the more stable isomer

[a] E_{a}-C = E[**TS-C**] − E[HP=PH$_3$] − E[OCXY]

[b] ΔE-IM = E[**IM**] − E[HP=PH$_3$] − E[OCXY]

[c] E_{a}-D = E[**TS-D**] − E[HP=PH$_3$] − E[OCXY]

[d] $\Delta E = E$[HP=CXY] + E[O=PH$_3$] − E[HP=PH$_3$] − E[OCXY]

[e] $\Delta E_{\mathrm{ST}} = E$(triplet) − E(singlet). A positive value indicate a singlet ground state

Since Ziegler et al. suggested that solvation strongly influences the middle part of the Wittig reaction of R$_2$C=PR′$_3$ + OCHR″ in DMSO [22]. We performed the self-consistent isodensity polarizable continuum model (SCI-PCM) to realize the solvent effect in this present study. Tetrahydrofuran (THF), one of the most common solvents used in Wittig or phospha-Wittig reactions [11], is chosen as the solvent and the dielectric constant ε is set to 7.58. As can be seen in Table 5, when comparing the system of HP=PH$_3$ + OCHX in the gas phase (see Table 2), these calculations in THF do not lead to significant changes in the relative energy for the products and there is still a reasonable correlation between the ΔE and the ΔE_{ST} values ($\Delta E = 0.6672 \times \Delta E_{\mathrm{ST}} - 58.0$, $R^2 = 0.9761$ from linear regression). Although Ziegler had suggested that the solvent may have chance to introduce a different intermediate [22], we still can locate the same four-membered intermediate for the phospha-Wittig reaction in THF. This conclusion conforms to the experimental result, which indicated the absence of betaine-like intermediates for the phospha-Wittig reaction [6].

4 Conclusions

In this study, we have investigated the energy profiles associated with the gas-phase phospha-Wittig reactions using a B3LYP approach with the 6-311++G** basis set. We have demonstrated that the computational results can be rationalized using a simple valence bond model, i.e., the CM model. In the present investigation, the CM model indicates the singlet–triplet splitting of OCHX as the key factor that determines the trend of the activation energies and the reaction enthalpy. In this study, we have shown that the singlet–triplet splitting in OCHX strongly correlates with their chemical reactivity. Furthermore, we have suggested that OCHX with more electro-releasing substituents

Table 5 B3LYP(SCI-PCM)/6-311++G** calculated singlet–triplet splittings (ΔE_{ST}, in kcal/mol) for OCHX and relative energies for the products (ΔE, in kcal/mol) for the reaction of $HP{=}PH_3 + OCHX \rightarrow HP{=}CHX + O{=}PH_3$ [X = H, F, Cl, CH_3, OCH_3, $N(CH_3)_2$, $C(CH_3)_3$] in THF ($\varepsilon = 7.58$)

X	ΔE^{a}	ΔE^{b}_{ST}
H	−15.4	66.5
CH_3		
E	*−8.8*	73.0
Z	−8.0	
$C(CH_3)_3$		
E	−8.0	72.1
Z	*−8.4*	
$N(CH_3)_2$		
E	*2.3*	88.1
Z	3.0	
Cl		
E	−2.7	82.5
Z	*−3.0*	
F		
E	*5.0*	94.8
Z	5.1	
OCH_3		
E	5.6	96.3
Z	*5.3*	

Values in italics indicate the data for the more stable isomer

[a] $\Delta E = E[HP{=}CHX] + E[O{=}PH_3] - E[HP{=}PH_3] - E[OCHX]$

[b] $\Delta E_{ST} = E(\text{triplet}) - E(\text{singlet})$. A positive value indicate a singlet ground state

will possess a smaller singlet–triplet splitting. This will facilitate the phospha-Wittig reaction and will result in a larger exothermicity. In spite of its simplicity, our approach provides a deeper insight and promises a solution of remaining problems.

In addition, the stereoselectivity of this phospha-Wittig reaction can be realized by the steric effect between the phosphorus ylide and OCHX. When the substituent on OCHX is large, *E*-form isomer is formed since this orientation can have the least steric hinderance between reactants. Moreover, we found that the reaction of $HP{=}PH_3$ with $OC(CH_3)_2$ is both kinetically and thermodynamically unfavorable because of the larger ΔE_{ST}. Additional investigations for the phospha-Wittig reactions with other ketones are currently in progress.

Acknowledgments The author is grateful to the National Center for High-performance Computing for computer time and facilities. The author also thank the National Science Council of Taiwan for financial support (NSC 97-2113-M-152-001-MY2) and Prof. Dr. San-Yan Chu for helpful and generous suggestions. Also, the author acknowledges the referees for their useful comments.

References

1. Maryanoff BE, Reitz AB (1989) Chem Rev 89:863–927. doi:10.1021/cr00094a007
2. Volatron F, Eisenstein O (1987) J Am Chem Soc 109:2–14. doi:10.1021/ja00235a001
3. Hoffmann RW (2001) Angew Chem Int Ed 40:1411–1416. doi:10.1002/1521-3773(20010417)40:8<1411::AID-ANIE1411>3.0.CO;2-U
4. Liao HY, Yen MY (2008) N J Chem 32:511–516. doi:10.1039/b715049k
5. Keith B, Dillon FM, Nixon JF (1998) Phosphorus: the carbon copy: from organophosphorus to phospha-organic chemistry. Wiley, Chichester
6. Shah S, Protasiewicz JD (2000) Coord Chem Rev 210:181–201. doi:10.1016/S0010-8545(00)00311-8
7. Marinetti A, Mathey F (1988) Angew Chem Int Ed Engl 27:1382–1384. doi:10.1002/anie.198813821
8. Marinetti A, Bauer S, Ricard L, Mathey F (1990) Organometallics 9:793–798. doi:10.1021/om00117a040
9. Marinetti A, Ricard L, Mathey F (1990) Organometallics 9:788–793. doi:10.1021/om00117a039
10. Shah S, Yap GPA, Protasiewicz JD (2000) J Organomet Chem 608:12–20. doi:10.1016/S0022-328X(00)00284-9
11. Shah S, Protasiewicz JD (1998) Chem Commun (Camb) 1585–1586. doi:10.1039/a802722f
12. Mracec M, Pascariu A, Berger S, Mracec M (2007) Int J Quantum Chem 107:1782–1793. doi:10.1002/qua.21298
13. Molander GA, Ham J, Canturk B (2007) Org Lett 9:821–824. doi:10.1021/ol063043e
14. El-Batta A, Jiang CC, Zhao W, Anness R, Cooksy AL, Bergdahl M (2007) J Org Chem 72:5244–5259. doi:10.1021/jo070665k
15. Robiette R, Richardson J, Aggarwal VK, Harvey JN (2006) J Am Chem Soc 128:2394–2409. doi:10.1021/ja056650q
16. Yu XC, Huang X (2002) Synlett 1895–1897
17. Lu WC, Wong NB, Zhang RQ (2002) Theor Chem Acc 107:206–210. doi:10.1007/s00214-001-0320-z
18. Balema VP, Wiench JW, Pruski M, Pecharsky VK (2002) J Am Chem Soc 124:6244–6245. doi:10.1021/ja017908p
19. Wang Q, El Khoury M, Schlosser M (2000) Chem Eur J 6:420–426. doi:10.1002/(SICI)1521-3765(20000204)6:3<420::AID-CHEM420>3.0.CO;2-H
20. Yamataka H, Nagase S (1998) J Am Chem Soc 120:7530–7536. doi:10.1021/ja974237f
21. Yamataka H, Nagareda K, Takatsuka T, Ando K, Hanafusa T, Nagase S (1993) J Am Chem Soc 115:8570–8576. doi:10.1021/ja00072a008
22. Seth M, Senn HM, Ziegler T (2005) J Phys Chem A 109:5136–5143. doi:10.1021/jp045318i
23. Smith RC, Chen XF, Protasiewicz JD (2003) Inorg Chem 42:5468–5470. doi:10.1021/ic0345471
24. Mathey F (2003) Angew Chem Int Ed 42:1578–1604. doi:10.1002/anie.200200557
25. Shah S, Simpson MC, Smith RC, Protasiewicz JD (2001) J Am Chem Soc 123:6925–6926. doi:10.1021/ja015767l
26. Power PP (1993) Angew Chem Int Ed Engl 32:850–851. doi:10.1002/anie.199308501
27. Cummins CC, Schrock RR, Davis WM (1993) Angew Chem Int Ed Engl 32:756–759. doi:10.1002/anie.199307561
28. Marinetti A, Ricard L, Mathey F (1992) Synthesis (Stuttgart) 1–2:157–162
29. Marinetti A, Lefloch P, Mathey F (1991) Organometallics 10:1190–1195. doi:10.1021/om00050a061
30. Becke AD (1993) J Chem Phys 98:5648–5652. doi:10.1063/1.464913

31. Becke AD (1992) J Chem Phys 97:9173–9177. doi:10.1063/1.463343
32. Becke AD (1992) J Chem Phys 96:2155–2160. doi:10.1063/1.462066
33. Lee CT, Yang WT, Parr RG (1988) Phys Rev B 37:785–789. doi:10.1103/PhysRevB.37.785
34. Krishnan R, Binkley JS, Seeger R, Pople JA (1980) J Chem Phys 72:650–654. doi:10.1063/1.438955
35. Frisch MJ, Pople JA, Binkley JS (1984) J Chem Phys 80:3265–3269. doi:10.1063/1.447079
36. Frisch MJ, Trucks GW, Schlegel HB, Scuseria GE, Robb MA, Cheeseman JR, Montgomery JA Jr, Vreven T, Kudin KN, Burant JC, Millam JM, Iyengar SS, Tomasi J, Barone V, Mennucci B, Cossi M, Scalmani G, Rega N, Petersson GA, Nakatsuji H, Hada M, Ehara M, Toyota K, Fukuda R, Hasegawa J, Ishida M, Nakajima T, Honda Y, Kitao O, Nakai H, Klene M, Li X, Knox JE, Hratchian HP, Cross JB, Adamo C, Jaramillo J, Gomperts R, Stratmann RE, Yazyev O, Austin AJ, Cammi R, Pomelli C, Ochterski JW, Ayala PY, Morokuma K, Voth GA, Salvador P, Dannenberg JJ, Zakrzewski VG, Dapprich S, Daniels AD, Strain MC, Farkas O, Malick DK, Rabuck AD, Raghavachari K, Foresman JB, Ortiz JV, Cui Q, Baboul AG, Clifford S, Cioslowski J, Stefanov BB, Liu G, Liashenko A, Piskorz P, Komaromi I, Martin RL, Fox DJ, Keith T, Al-Laham MA, Peng CY, Nanayakkara A, Challacombe M, Gill PMW, Johnson B, Chen W, Wong MW, Gonzalez C, Pople JA (2003) Gaussian 03. Gaussian, Inc, Pittsburgh
37. Baerends EJ, Gritsenko OV (1997) J Phys Chem A 101:5383–5403. doi:10.1021/jp9703768
38. Laird BB, Ross RB, Ziegler T (eds) (1996) Chemical applications of density-functional theory. American Chemical Society, Washington
39. Glendening ED, Reed AE, Carpenter JE, Weinhold F (1996) NBO 4.0. Theoretical Chemistry Institute, University of Wisconsin, Madison
40. Foresman JB, Keith TA, Wiberg KB, Snoonian J, Frisch MJ (1996) J Phys Chem 100:16098–16104. doi:10.1021/jp960488j
41. Hammond GS (1955) J Am Chem Soc 77:334–338. doi:10.1021/ja01607a027
42. Shaik SS, Schlegel HB, Wolfe S (1992) Theoretical aspects of physical organic chemistry: the Sn2 mechanism. Wiley, New York
43. Su MD, Liao HY, Chung WS, Chu SY (1999) J Org Chem 64:6710–6716. doi:10.1021/jo990504j